Issue No. 3 · 2026
ADVANCED STUDIES
IN ARCHITECTURE AND CIVIL ENGINEERING
(ASACE)

ISSN 3134-8475 (Print)
ISSN 3134-8483 (Online)

UDC 697.13
Research article
https://doi.org/10.51488/3134-8483/3-05

CC BY 4.0

SEPARATING EXTERIOR AND DEEP-GROUND TEMPERATURE RESPONSES IN HEAT-LOSS CALCULATION FOR A BASEMENT FLOOR WITH INDIRECT INSULATION

Kuralay K. Ramazan[1]*, Sayat E. Niyetbay[1]

[1]International Educational Corporation, 050043, Almaty, Kazakhstan
*Corresponding author, e-mail: kuralayy07@gmail.com

ABSTRACT

Introduction. Ground-contact floors exchange heat with both exterior conditions and deeper soil. A correction calibrated against one indoor–outdoor temperature difference may therefore lose accuracy when the deep-ground temperature changes. This study develops a transparent two-response calculation for a basement floor with indirect wall insulation. **Materials and Methods.** A two-dimensional, steady-state finite-volume model represented a 7.45 m floor strip located 4.15 m below ground level. Five insulation depths between 1.50 and 4.15 m were investigated at a constant thickness of 100 mm. Separate unit-temperature calculations identified exterior and deep-ground response coefficients. Three depths supplied interpolation anchors; two intermediate depths were kept for checking. Mesh refinement, energy balance and boundary-condition sensitivity were evaluated. **Results and Discussion.** At the reference temperatures, increasing insulation depth reduced combined floor–wall heat flow from 60.1 to 46.9 W/m, while floor heat flow increased from 20.49 to 23.02 W/m. Each further metre of insulation depth saved less, from about 6.6 to 4.3 W/m per metre. Scalar interpolation reproduced intermediate reference cases within 0.33%, but errors reached −10.73% and +13.46% in two changed-temperature checks. Interpolating the two response coefficients reduced these errors to +0.20% and +0.33%. Carrying a scalar correction between indicative design conditions of Almaty and Astana shifted floor heat flow by about 8%. The wall heat flow was not yet in the asymptotic mesh range, and soil conductivity and deep-ground temperature affected the result more than interpolation error did. **Conclusions.** Keeping the two thermal driving differences separate lets the reduced calculation be transferred across boundary temperatures and climates within the linear model. Other geometries, transient modelling and field measurements are still needed.

KEYWORDS: ground-floor heat loss; basement; indirect insulation; superposition; response coefficients; zonal method.

FOR CITATION:

Ramazan K.K., Niyetbay S.E. Separating exterior and deep-ground temperature responses in heat-loss calculation for a basement floor with indirect insulation. Advanced Studies in Architecture and Civil Engineering. 2026; 1 (3): 91-105. https://doi.org/10.51488/3134-8483/3-05

© Ramazan K. K., Niyetbay S. E., 2026

Issue No. 3 · 2026
ADVANCED STUDIES
IN ARCHITECTURE AND CIVIL ENGINEERING
(ASACE)

ISSN 3134-8475 (Print)
ISSN 3134-8483 (Online)

ӘОЖ 697.13
Ғылыми мақала
https://doi.org/10.51488/3134-8483/3-05

CC BY 4.0

ЖАНАМА ОҚШАУЛАНҒАН ЖЕРТӨЛЕ ЕДЕНІ АРҚЫЛЫ ЖЫЛУ ШЫҒЫНЫН ЕСЕПТЕУДЕ СЫРТҚЫ АУА МЕН ТЕРЕҢ ТОПЫРАҚ ТЕМПЕРАТУРАЛАРЫНЫҢ ӘСЕРІН БӨЛЕК ЕСКЕРУ

Құралай Қ. Рамазан[1*], Саят Е. Ниетбай[1]

[1]Халықаралық білім беру корпорациясы, 050043, Алматы, Қазақстан
*Хат-хабар автор, e-mail: kuralayy07@gmail.com

АҢДАТПА

Кіріспе. Топырақпен жанасатын едендер сыртқы ортамен және терең топырақ қабаттарымен жылу алмасады. Сондықтан тек ішкі және сыртқы ауа температураларының айырмасына негізделген түзету терең топырақ температурасы өзгерген кезде дәлдігін жоғалтуы мүмкін. Зерттеудің мақсаты - қабырғасы жанама оқшауланған жертөле едені үшін екі температуралық әсерді жеке ескеретін түсінікті есептеу тәсілін әзірлеу. **Материалдар мен әдістер.** Екіөлшемді стационарлық ақырлы көлемдер моделі жер бетінен 4,15 м тереңдікте орналасқан, ені 7,45 м еден жолағын сипаттады. Оқшаулаудың қалыңдығы 100 мм болып сақталып, оның 1,50–4,15 м аралығындағы бес тереңдігі қарастырылды. Сыртқы орта мен терең топырақтың әсер коэффициенттері температураны бірлік шамаға өзгерту арқылы жеке анықталды. Үш тереңдік интерполяцияның тірек нүктелері ретінде пайдаланылды, ал екі аралық тереңдік тексеруге қалдырылды. **Нәтижелер және талқылау.** Бастапқы температуралар кезінде оқшаулауды тереңдету еден мен қабырғаның қосынды жылу ағынын 60,1-ден 46,9 Вт/м-ге төмендетті. Осы кезде еденнің жеке ағыны 20,49-дан 23,02 Вт/м-ге артты. Оқшаулауды әрбір келесі метрге тереңдетудің пайдасы азаяды: тереңдіктің бір метріне шаққанда шамамен 6,6-дан 4,3 Вт/м-ге дейін. Бір коэффициентпен интерполяциялау бастапқы аралық есептерді 0,33% шегінде қайталады, бірақ температуралары өзгертілген екі тексеруде қателік −10,73% және +13,46% болды. Екі әсер коэффициентін жеке интерполяциялау қателіктерді +0,20% және +0,33% шамаларына дейін азайтты. Бір скалярлық түзетуді Алматы мен Астананың болжамды есептік жағдайлары арасында ауыстыру еден арқылы өтетін ағынды шамамен 8%-ға өзгертеді. **Қорытынды.** Екі температуралық айырманы бөлек қарастыру ықшам есепті сызықтық модель шегінде басқа шекаралық температуралар мен климаттық жағдайларға көшіруге мүмкіндік береді.

ТҮЙІН СӨЗДЕР: топырақтағы еден арқылы жылу шығыны; жертөле; жанама оқшаулау; суперпозиция; әсер коэффициенттері; аймақтық әдіс.

ДӘЙЕКСӨЗ ҮШІН:

Рамазан Қ.Қ., Ниетбай С.Е. жанама оқшауланған жертөле едені арқылы жылу шығынын есептеуде сыртқы ауа мен терең топырақ температураларының әсерін бөлек ескеру. Advanced Studies in Architecture and Civil Engineering. 2026; 1 (3): 91-105. https://doi.org/10.51488/3134-8483/3-05

© Рамазан Қ.Қ., Ниетбай С.Е., 2026

Issue No. 3 · 2026
ADVANCED STUDIES
IN ARCHITECTURE AND CIVIL ENGINEERING
(ASACE)

ISSN 3134-8475 (Print)
ISSN 3134-8483 (Online)

УДК 697.13
Научная статья
https://doi.org/10.51488/3134-8483/3-05

CC BY 4.0

РАЗДЕЛЬНЫЙ УЧЁТ ВЛИЯНИЯ НАРУЖНОЙ ТЕМПЕРАТУРЫ И ТЕМПЕРАТУРЫ ГЛУБИННОГО ГРУНТА ПРИ РАСЧЁТЕ ТЕПЛОПОТЕРЬ ЧЕРЕЗ ПОЛ ПОДВАЛА С КОСВЕННЫМ УТЕПЛЕНИЕМ

Куралай К. Рамазан[1*], Саят Е. Ниетбай[1]

[1]Международная образовательная корпорация, 050043, Алматы, Казахстан
*Автор-корреспондент, e-mail: kuralayy07@gmail.com

АННОТАЦИЯ

Введение. Полы, контактирующие с грунтом, обмениваются теплом как с наружной средой, так и с глубинными слоями грунта. Поэтому поправка, определённая через одну разность внутренней и наружной температур, может терять точность при изменении температуры глубинного грунта. Цель исследования – разработать прозрачный расчёт пола подвала с косвенным утеплением стены на основе двух температурных откликов. **Материалы и методы.** Двумерная стационарная модель конечных объёмов описывала полосу пола шириной 7,45 м на глубине 4,15 м. Рассмотрены пять глубин утепления от 1,50 до 4,15 м при постоянной толщине 100 мм. Отдельными расчётами с единичным изменением температуры определены коэффициенты влияния наружной среды и глубинного грунта. Три глубины использованы как опорные точки интерполяции, две промежуточные оставлены для проверки. Оценены сеточная сходимость, энергетический баланс и чувствительность к граничным условиям. **Результаты и обсуждение.** При исходных температурах увеличение глубины утепления снизило суммарный поток через пол и стену с 60,1 до 46,9 Вт/м, тогда как поток через пол вырос с 20,49 до 23,02 Вт/м. Отдача каждого следующего метра утепления убывает: примерно с 6,6 до 4,3 Вт/м на метр глубины. Интерполяция одного коэффициента воспроизводила промежуточные исходные случаи с отклонением до 0,33%, однако в двух проверках с изменёнными температурами ошибки составили −10,73% и +13,46%. Раздельная интерполяция двух коэффициентов снизила ошибки до +0,20% и +0,33%. Перенос скалярной поправки между ориентировочными расчётными условиями Алматы и Астаны искажает поток через пол примерно на 8%. Поток через стену при сгущении сетки ещё не вышел на асимптотический режим, а теплопроводность грунта и температура нижней границы влияют на результат сильнее, чем ошибка интерполяции. **Выводы.** Раздельный учёт двух температурных воздействий позволяет переносить сокращённый расчёт на другие граничные температуры и климатические условия в рамках линейной модели.

КЛЮЧЕВЫЕ СЛОВА: теплопотери через пол по грунту; подвал; косвенное утепление; суперпозиция; коэффициенты отклика; зональный метод.

ДЛЯ ЦИТИРОВАНИЯ:

Рамазан К.К., Ниетбай С.Е. раздельный учёт влияния наружной температуры и температуры глубинного грунта при расчёте теплопотерь через пол подвала с косвенным утеплением. Advanced Studies in Architecture and Civil Engineering. 2026; 1 (3): 91-105. https://doi.org/10.51488/3134-8483/3-05

© Рамазан К.К., Ниетбай С.Е., 2026

ISSN 3134-8475 (Print)
ISSN 3134-8483 (Online)

1 INTRODUCTION

Ground-contact floors require a calculation that represents the surrounding soil as well as the construction layers. ISO 13370 separates ground heat transfer from ordinary above-ground envelope calculations [1], whereas ISO 10211 provides the framework for detailed two- and three-dimensional thermal-bridge calculations [2]. The practical difficulty is to translate a spatial heat-conduction solution into a short engineering calculation without concealing the environmental assumptions that determine the result.

The reviews by Rees et al. [3] and Zoras [4] describe analytical, numerical and simplified approaches and show why soil properties and geometric representation matter. These studies provide the physical background rather than validation data for the present model. Moisture-dependent properties, three-dimensional edges and long thermal time constants complicate the relationship between an instantaneous air-temperature difference and heat transfer through a ground-contact floor.

For indirect insulation, the insulation is located on the adjacent underground wall rather than continuously below the slab. Malyavina et al. [5] expressed detailed calculations through equivalent ground-floor resistances. Gnezdilova [6] developed this approach using an annual unsteady soil–construction model, including an implicit scheme and treatment of freezing and thawing. These works motivate retaining the coupled floor–wall–soil domain. Their reported experimental results and annual thermal resistances are not adopted as measurements of the present section.

The Kiva framework demonstrates how detailed foundation calculations can be organised efficiently [7]. Its reduction of three-dimensional foundation effects to two-dimensional representations also highlights the importance of exposed perimeter and footprint geometry [8]. A straight unit-length section is therefore useful for studying a mechanism, but is not automatically a whole-building model. Diagnostic benchmarks such as IEA BESTEST provide a separate route for assessing ground-coupled solvers [9]; passing those benchmarks is not claimed here.

This study addresses a narrower question: can a correction based on one indoor–outdoor temperature difference remain accurate when a separate deep-ground boundary temperature changes? The working hypothesis is that a single multiplier mixes two independent thermal drivers. A linear steady-state model allows those drivers to be retained explicitly through two response coefficients. This is an application of linear superposition, not a new heat-conduction law.

The contribution is a reproducible calculation for an idealised basement section: five insulation depths are analysed, three supply interpolation anchors, and the remaining two are used for checks. A two-response reduction is compared with a conventional scalar correction at reference and changed temperatures, and also between design conditions of two Kazakhstan cities. The question matters for Kazakhstan, where exterior design temperatures and ground temperatures differ widely from south to north, yet ground-floor losses are still usually estimated with the zonal procedure described in Section 2.3. Numerical consistency, interpolation error and sensitivity are reported separately, and the limitations of the study are collected in Section 3.5.

2 METHODS AND MATERIALS

2.1 Geometry, properties and boundary conditions

The section in Fig. 1 uses a 7.45 m floor strip and a floor level 4.15 m below exterior ground. These dimensions are typical of a residential basement and are used here as a numerical idealisation; wall and slab thicknesses are assumed. Exterior vertical insulation terminates at depth d, and the floor has no continuous underside insulation. The right-hand vertical boundary at x = 7.45 m is adiabatic and is taken as the plane of symmetry

Issue No. 3 · 2026
ADVANCED STUDIES
IN ARCHITECTURE AND CIVIL ENGINEERING
(ASACE)
ISSN 3134-8475 (Print)
ISSN 3134-8483 (Online)

of the building, so the strip represents half of a floor 14.9 m wide. For a long building of this width the characteristic floor dimension of ISO 13370, B′ = A/(0.5P), approaches the floor width, B′ ≈ 14.9 m [1]. Per-metre results can therefore be compared with ISO 13370 and scaled by the building length, with corners treated separately

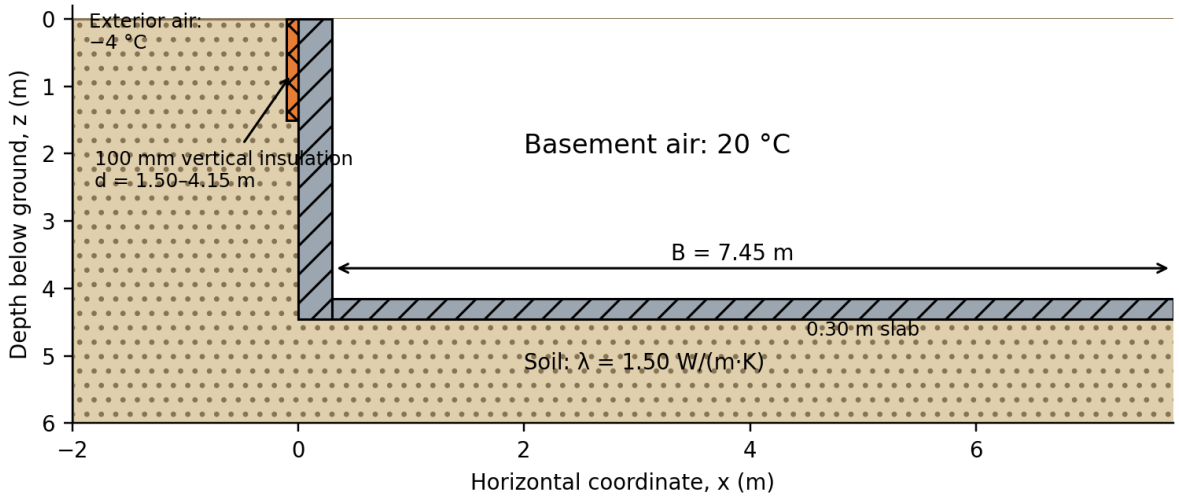

Fig. 1. Idealised floor–wall–soil section. The visible crop excludes the distant boundaries; the computation extends 10 m outward and 14 m downward

Table 1. Inputs used in the stationary calculation

Quantity	Value	Status
Floor depth / width	4.15 / 7.45 m	Geometric idealisation
Wall / slab thickness	0.30 / 0.30 m	Assumed
Insulation thickness / depth	0.10 m / 1.50–4.15 m	Five numerical variants
λ: concrete / soil / insulation	1.70 / 1.50 / 0.040 W/(m·K)	Fixed assumptions
Indoor / exterior / bottom T	20 / −4 / 10 °C	Reference scenario
Rs: floor / wall / ground surface	0.17 / 0.13 / 0.04 m²·K/W	Prescribed film resistances
Exterior extent / bottom depth	10 / 14 m	Finite-domain scenario

Material properties are not product certificates or site measurements. ISO 10456 provides procedures for declared and design thermal values [10]; application requires material-specific information. ISO 6946 supports layer-resistance calculations but excludes components involving ground heat transfer [11]. Accordingly, the insulation resistance δ/λ = 2.50 m²·K/W is not added to the entire floor area. The two-dimensional domain determines which heat paths interact with the wall insulation.

The soil domain extends 10 m beyond the wall and 14 m below ground, and the bottom boundary has a fixed temperature Td = 10 °C. ISO 10211 recommends a considerably larger ground region, of the order of 2.5b in each direction, where b is the floor width [2]; for b = 14.9 m this is about 37 m. The prescribed bottom temperature is therefore a physical input of the model and not only a numerical cut-off. Below the layer of seasonal fluctuations, ground temperature is close to the mean annual temperature of the ground

Issue No. 3 · 2026
ADVANCED STUDIES
IN ARCHITECTURE AND CIVIL ENGINEERING
(ASACE)
ISSN 3134-8475 (Print)
ISSN 3134-8483 (Online)

surface, which is usually one to three kelvin above the mean annual air temperature. The mean annual air temperature is about 10 °C in Almaty and about 3–4 °C in Astana [12], so Td = 10 °C corresponds to southern conditions of the Almaty type. The reference exterior temperature Te = −4 °C is treated as a mean temperature of the heating period. The influence of domain size and of the bottom condition is discussed in Section 3.4.

2.2 Governing equations and discretisation

The stationary problem assumes constant isotropic conductivity, no internal heat sources, perfect material contact and no groundwater advection. The governing equation is:

$$\nabla \cdot (\lambda \nabla T) = 0 \qquad (1)$$

The normal heat flux density qn is in W/m². Floor heat flow per unit wall length Q′F is obtained by integrating over the floor width B:

$$q_n = -\lambda \frac{\partial T}{\partial n}, \qquad Q'_F = \int_0^B q_F(x)\,dx \quad (2)$$

A cell-centred finite-volume balance uses series resistances between adjacent cell centres [13]. For a one-metre-long section, GPN is a face conductance in W/K; δP and δN are the half-cell distances and APN is the face area. The discrete equation is:

$$G_{PN} = \frac{A_{PN}}{\delta_P/\lambda_P + \delta_N/\lambda_N}, \qquad \sum_N G_{PN}(T_P - T_N) + \sum_b G_{Pb}(T_P - T_b) = 0 \quad (3)$$

The mesh follows material boundaries and the end of each insulation strip. This conservative formulation is related to difference schemes for diffusion problems [14]. Exterior and interior exposed surfaces use film resistances; the bottom has prescribed temperature Td. The distant vertical edges and wall-top cut are adiabatic. Heat entering the domain is positive at a boundary. Here Tb is the air temperature on the exposed side of the boundary (Ti indoors, Te at the exterior ground surface), and Ts is the corresponding surface temperature:

$$q_b = \frac{T_b - T_P}{R_s + \delta_P/\lambda_P}, \qquad T_s = T_b - q_b R_s \quad (4)$$

The sparse linear system is assembled in Python using NumPy [15] and solved with SciPy [16]. Matplotlib generates all numerical figures [17]. Nominal mesh spacings of 0.20, 0.10 and 0.05 m are compared, with local segment widths adjusted to fit interfaces. No fitted thermal conductivity is inferred from camera images. Under the linear assumptions, separate temperature responses can be combined by superposition, consistent with classical conduction theory [18].

2.3 Simplified reference and scalar correction

For comparison, the zonal method of Russian design practice is used, which goes back to SNiP 2.04.05-91* [19, Appendix 9]. The buried wall and the floor are divided into 2 m strips counted from the ground surface along the buried wall, with standard resistances RI = 2.1, RII = 4.3, RIII = 8.6 and RIV = 14.2 m²·K/W. With a buried depth of 4.15 m, zones I and II and the first 0.15 m of zone III lie on the wall. The floor strip therefore receives the remaining 1.85 m of zone III (RIII) and 5.60 m of zone IV (RIV). In Kazakhstan, thermal requirements for the envelope are set by SP RK 2.04-107-2013 [20], and heat losses through floors on the ground are in practice still calculated by this zonal procedure. The resistances are comparison inputs, not material resistances or an ISO 13370 result. At Ti − Te = 24 K:

$$Q'_{\text{zone}} = (T_i - T_e)\left(\frac{1.85}{8.6} + \frac{5.60}{14.2}\right) = 14.6276\ \text{W/m} \qquad (5)$$

A scalar correction k is calibrated at d = 1.50, 2.50 and 4.15 m and linearly interpolated. The 2.00 and 3.50 m cases are withheld from the interpolation anchors.

$$k(d) = \frac{Q'_{F,2D}(d)}{Q'_{\text{zone}}}, \qquad \hat{k}(d) = k_1 + \frac{d - d_1}{d_2 - d_1}(k_2 - k_1) \quad (6)$$

3 RESULTS AND DISCUSSION

3.1 Coupled floor and wall heat transfer

Fig. 2 shows the calculated field for the reference case, d = 1.50 m. The image is a numerical temperature map, not a thermogram. Temperature gradients and surface heat flux are largest near the junction. The dashed line marks the boundary between the two

Issue No. 3 · 2026
ADVANCED STUDIES
IN ARCHITECTURE AND CIVIL ENGINEERING
(ASACE)
ISSN 3134-8475 (Print)
ISSN 3134-8483 (Online)

comparison strips; it is not a discontinuity in the material or in the solved temperature field.

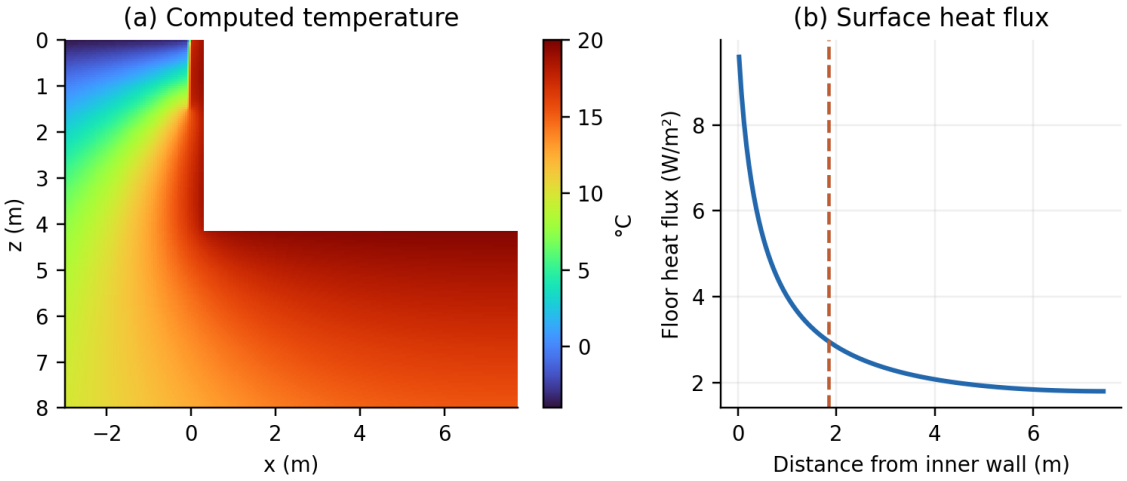

Fig. 2. Reference stationary temperature field and floor heat-flux profile. Input temperatures are prescribed scenarios.

Table 2. Heat flows at Ti = 20 °C, Te = −4 °C and Td = 10 °C

d (m)	Q′F (W/m)	Q′W (W/m)	Sum (W/m)	k
1.50	20.49	39.6	60.1	1.4008
2.00	20.73	36.1	56.8	1.4170
2.50	21.05	33.1	54.1	1.4393
3.50	22.17	27.5	49.6	1.5157
4.15	23.02	23.8	46.9	1.5735

Extending vertical insulation from 1.50 to 4.15 m decreases the combined heat flow by 22.0%, while the floor contribution increases by 12.3% and the wall contribution decreases by 39.8%. Insulating the wall reshapes the shared soil temperature field and redistributes heat between surfaces, so the floor component need not fall. A design comparison based only on the floor component would misread the combined benefit.

Table 2 also shows that each additional metre of insulation depth is worth less than the previous one. Moving the end of the insulation from 1.50 to 2.50 m reduces the combined flow by 6.0 W/m, that is, about 6 W/m per metre of depth. The next 1.65 m, from 2.50 to 4.15 m, give 7.3 W/m, or about 4.4 W/m per metre. Interval by interval the specific saving falls from 6.6 W/m per metre (1.50–2.00 m) to 5.4, 4.5 and 4.3 W/m per metre, while the amount of insulation grows linearly with depth (0.1 m³ per metre of depth and metre of wall). A reasonable design depth is therefore the one at which the seasonal energy saving of the next metre no longer pays for the extra insulation and excavation. That comparison needs local prices and degree-days and is not made here, but the diminishing return itself follows from the coupled field and is likely to appear in other sections of this type.

The prescribed zonal reference underestimates the modelled floor flow by 28.61–36.45%. This difference belongs to the defined comparison and boundary conditions; it is not a universal error of all zonal methods. Scalar interpolation at the two withheld depths gives +0.220% and +0.327% relative errors. The error measure used throughout is:

$$\varepsilon = 100\,\frac{Q'_{\mathrm{pred}} - Q'_{F,2D}}{Q'_{F,2D}} \qquad (7)$$

ISSN 3134-8475 (Print)
ISSN 3134-8483 (Online)

Agreement of this kind concerns only the numerical model itself; uncertainty of the inputs is examined in Section 3.3.

3.2 Two-response reduction and changed-temperature tests

For fixed geometry, conductivities and film resistances, the linear problem gives a floor-flow response to two independent temperature differences:

$$Q'_F = a(d)(T_i - T_e) + b(d)(T_i - T_d) \quad (8)$$

Here a and b have units W/(m·K). The coefficients are found by keeping the indoor boundary at 20 °C and applying two separate unit-difference load cases; arguments below are ordered Ti, Te, Td:

$$a = \frac{Q'_F(20,19,20)}{1\ \mathrm{K}}, \qquad b = \frac{Q'_F(20,20,19)}{1\ \mathrm{K}} \quad (9)$$

The coefficients are interpolated independently between the same three depths used for scalar calibration:

$$\hat{a}(d) = a_1 + \frac{d - d_1}{d_2 - d_1}(a_2 - a_1),$$
$$\hat{b}(d) = b_1 + \frac{d - d_1}{d_2 - d_1}(b_2 - b_1) \quad (10)$$

Table 3. Response coefficients and their role in the interpolation

d (m)	a (W/(m·K))	b (W/(m·K))	Role
1.50	0.324464	1.270292	Anchor
2.00	0.334017	1.271016	Withheld check
2.50	0.347006	1.272606	Anchor
3.50	0.389316	1.282764	Withheld check
4.15	0.419101	1.295855	Anchor

A single apparent coefficient hides the ratio of the two driving differences. Rearranging Eq. (8) makes this dependence explicit:

$$H'_{\mathrm{eff}} = \frac{Q'_F}{T_i - T_e} = a + b\frac{T_i - T_d}{T_i - T_e} \quad (11)$$

Consequently, k calibrated at one ratio is not generally transferable to a different Td or Te. By contrast, the exact coefficients a and b reproduce the linear discrete solution at a given geometry. Interpolation across depth introduces approximation error; superposition at an anchor depth is a consistency test rather than independent proof of predictive accuracy.

Table 4. Additional direct numerical checks with changed temperatures

Case: d; Te; Td	2D Q′F	Scalar Q′F / ε	Two-response Q′F / ε
V1: 1.50; −3; 10	20.166	19.636 / −2.625%	20.166 / <0.001%
V2: 2.00; −10; 5	29.086	25.965 / −10.729%	29.144 / +0.200%
V3: 3.50; 5; 15	12.254	13.902 / +13.456%	12.294 / +0.330%

Depths are in metres, temperatures in °C and heat flows in W/m. Ti remains 20 °C. V2 and V3 test both withheld geometry and changed temperatures. The numerical reference was solved directly rather than generated from the interpolated coefficients.

The temperatures of V1–V3 were chosen to stress the formula rather than to represent design conditions; V3 (Te = 5 °C, Td = 15 °C) in particular has no direct climatic counterpart. A more practical test is to move a correction from one climate to another. Table 5 uses indicative pairs of design exterior temperature and deep-ground temperature for Almaty and Astana [12]. Because 1.50, 2.50 and 4.15 m are anchor depths, the exact coefficients of Table

ISSN 3134-8475 (Print)
ISSN 3134-8483 (Online)

3 reproduce the direct solution at these depths (see V1), and Eq. (8) gives Q′F without further runs. The scalar coefficient H′eff = Q′F/(Ti − Te) is calibrated for one city and applied to the other

Table 5. Transfer of a scalar correction between indicative design conditions (Ti = 20 °C; Almaty: Te = −20 °C, Td = 10 °C; Astana: Te = −31 °C, Td = 5 °C)

d (m)	Q′F, Almaty / Astana (W/m)	ε, Almaty → Astana	ε, Astana → Almaty
1.50	25.68 / 35.60	−8.0%	+8.7%
2.50	26.61 / 36.79	−7.8%	+8.4%
4.15	29.72 / 40.81	−7.1%	+7.7%

A designer who carries a single correction from Almaty to Astana would underestimate the floor heat flow by 7–8%, and in the opposite direction would overestimate it by 8–9%. The error is smaller than in V2 and V3 because the ratio (Ti − Td)/(Ti − Te) changes only from 0.25 to 0.29 between the two cities, yet it is still more than twenty times the interpolation error of the two-response method.

The reference pair of Table 2 is a separate case: k calibrated at Te = −4 °C and applied to the Almaty design pair would overestimate Q′F by 29–33% at the three anchor depths. If other climatic data are adopted, Table 5 should be recalculated from Eq. (8) and Table 3.

3.3 Numerical checks and parameter sensitivity

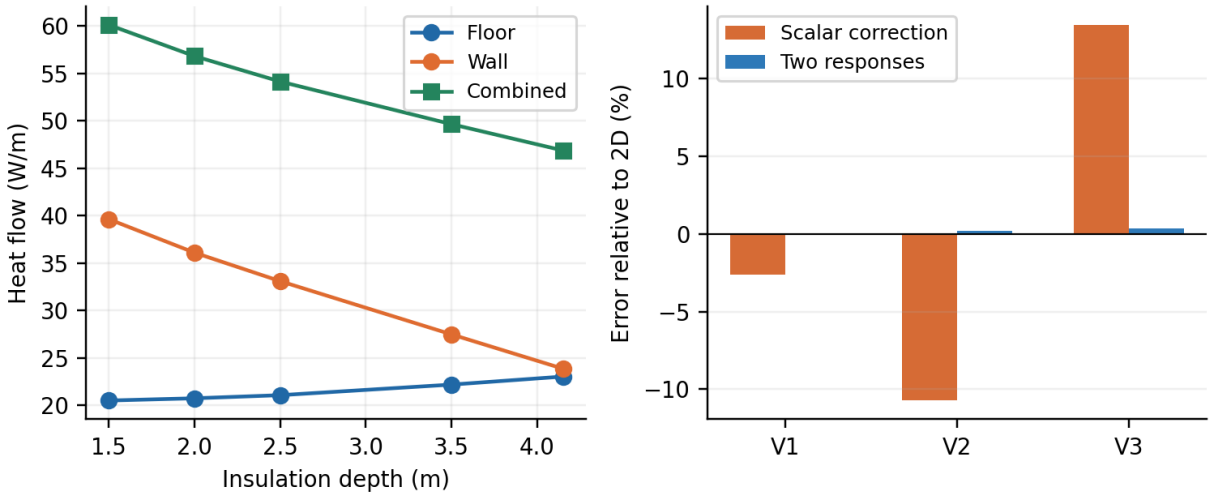

Fig. 3. (a) Redistribution of floor and wall heat flows; (b) errors in the additional temperature checks from Table 4.

The improved agreement in V2 and V3 follows from preserving two boundary responses rather than forcing both through Ti – Te. It should not be interpreted as a general accuracy of 0.33% for ground heat-loss prediction. At the reference temperatures, scalar and two-response interpolation are algebraically equivalent because both use the same anchors. Their distinction appears when the temperature ratio changes.

Issue No. 3 · 2026
ADVANCED STUDIES
IN ARCHITECTURE AND CIVIL ENGINEERING
(ASACE)
ISSN 3134-8475 (Print)
ISSN 3134-8483 (Online)

Table 6. Mesh comparison for d = 1.50 m

Nominal h (m)	Active cells	Q′F (W/m)	Q′W (W/m)
0.20	5,716	20.5030	38.9459
0.10	21,948	20.4970	39.2356
0.05	87,239	20.4900	39.6210

The floor integral is insensitive to the mesh (Table 6): it changes by 0.006 and 0.007 W/m between successive levels, about 0.03%. The wall flow behaves differently. Its increments are 0.29 and 0.39 W/m, so the second refinement changes the result more than the first. With a refinement ratio r = 2, the observed order $p = \ln(\varepsilon 21/\varepsilon 32)/\ln r$ is negative, $p \approx -0.41$. The wall solution is therefore not yet in the asymptotic range, and Richardson extrapolation and the grid convergence index (GCI) [21] cannot be applied formally. The most likely cause is the singular behaviour near the wall–floor corner and at the end of the insulation strip. The floor series also gives $p < 0$, but its total spread is 0.013 W/m and has no practical effect. For this reason wall flows and floor–wall sums in Table 2 are given to 0.1 W/m. If a wall-flow uncertainty of ±0.4 W/m (about 1%, the size of the last increment) is assumed independently at 1.50 and 4.15 m, the reduction in combined heat flow lies between about 20.8% and 23.2%; the conclusion of a reduction of about 22% does not depend on the mesh qualitatively.

3.4 Physical interpretation and measurement requirements

A further local refinement near the junction (for example, h = 0.025 m within about 0.5 m of the corner and of the insulation end) or a four-level GCI estimate is to be added by the authors. Minimum surface temperatures for condensation checks would also require this refinement.

The absolute energy-balance residual is below 3×10^{-10} W/m in the unit-response calculations. A separate one-dimensional slab check gives 38.7244 W/m² by both the analytical series-resistance expression and the discrete calculation. This checks the face-resistance implementation; it does not replace a full multidimensional benchmark or field comparison.

Sensitivity tests keep d = 1.50 m. Changing soil conductivity from 1.50 to 1.00 or 2.00 W/(m·K) changes floor flow by −32.06% or +30.77%. Changing Td from 10 to 5 or 15 °C changes floor flow by approximately +31.00% or −31.00%. Thus, input uncertainty is much larger than the reduction error in the tested interpolation range.

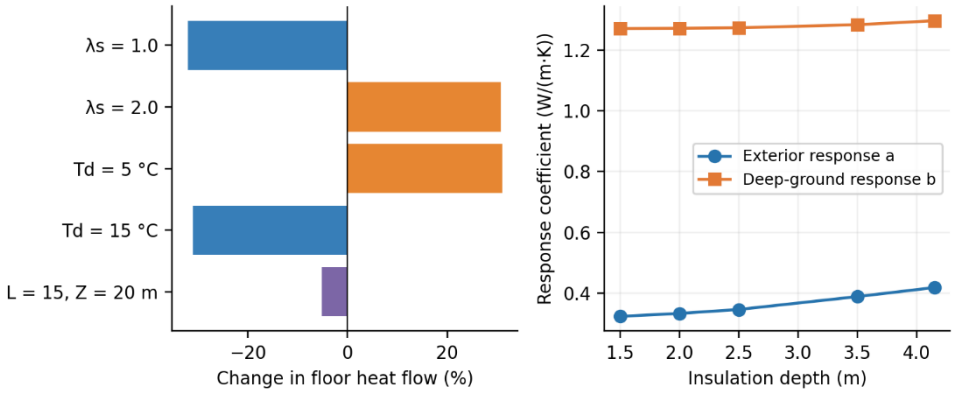

Fig. 4. (a) Sensitivity of the reference floor flow; (b) the two boundary-response coefficients. The expanded-domain case also moves the prescribed bottom-temperature boundary

ISSN 3134-8475 (Print)
ISSN 3134-8483 (Online)

The expanded domain extends 15 m outward and 20 m downward and gives 19.429 W/m, 5.18% below the reference. Because the fixed 10 °C boundary is moved deeper, the test changes the boundary-value problem as well as its size, and it does not show convergence to an infinite soil domain. The change is an order of magnitude larger than the interpolation error. Since the deep-ground term supplies about 62% of the floor flow, the bottom condition largely sets the absolute result. The method comparison is less affected, because the scalar and two-response reductions are tested against direct solutions on the same domain, but the absolute flows are. Result for an adiabatic bottom boundary at about 2.5b (≈ 37 m) with a horizontal extent of the same order: Q′F = … W/m, difference from the reference … % (to be added by the authors).

At d = 1.50 m, the deep-ground contribution b(Ti − Td) is about 62.0% of floor flow in the reference scenario. The coefficient b varies little across the five depths, whereas a increases more strongly. The response coefficients are algebraic sensitivities to prescribed boundaries: they should not be described as a measured separation of actual heat paths in the soil.

Field validation requires synchronised measurements tied to coordinates on the section. ISO 9869-1 describes heat-flow-meter measurements for building components with predominantly one-dimensional heat flow [22]; its assumptions must be considered near a junction. ISO 6781-1 addresses infrared inspection procedures [23]. Nardi et al. [24] and Song et al. [25] distinguish temperature mapping from quantitative thermal-transmittance assessment and discuss the additional conditions required for reliable interpretation.

The proposed reduction is intended for a prescribed unit-length section. It cannot be multiplied by an arbitrary building perimeter without accounting for footprint area, exposed boundaries and corners. The EnergyPlus implementation of Foundation:Kiva explicitly uses area and exposed perimeter to construct representative sections [26]. That geometric reduction is not implemented in the present model.

3.5 Limitations

The results refer to the numerical model of Section 2 and have the following limitations. They are not a field validation: no measured temperatures or heat flows were used for calibration or comparison. The calculation is stationary, so annual energy use, soil heat storage, moisture and freezing are not represented. Only one straight section and one insulation scheme are studied, 100 mm vertical wall insulation without insulation under the slab; corners, other thicknesses and underslab insulation are left for later work. Material properties are assumed rather than certified or measured. The finite domain with a prescribed bottom temperature controls the absolute floor flow (Section 3.4), and the wall flow is not mesh-converged in the asymptotic sense (Section 3.3). Finally, the response coefficients are algebraic sensitivities to boundary temperatures and should not be read as a measured split of heat paths in the soil. Within these limits the comparison of the scalar and two-response reductions remains internally consistent, since both are checked against the same direct solutions.

4 CONCLUSION

The stationary study evaluated five depths of 100 mm vertical wall insulation in a defined basement floor–wall–soil section. Extending the insulation from 1.50 to 4.15 m reduced combined floor–wall heat flow from 60.1 to 46.9 W/m, by about 22%, while floor flow increased from 20.49 to 23.02 W/m as the coupled temperature field changed. The saving per additional metre of depth fell from about 6.6 to 4.3 W/m, which gives a basis for an economic choice of insulation depth.

1. The calculation was refined by retaining separate exterior-air and deep-ground temperature responses. At two

ISSN 3134-8475 (Print)
ISSN 3134-8483 (Online)

withheld insulation depths and changed boundary temperatures, the scalar correction deviated from the direct numerical solution by −10.73% and +13.46%, whereas the two-response interpolation gave +0.20% and +0.33%. Moving a scalar correction between the indicative design conditions of Almaty and Astana changed the floor flow by about 8%. This shows better agreement within the specified linear model; the superposition principle itself is not claimed as new.

2. Changes in assumed soil conductivity and deep-ground temperature affected floor flow by about 31–32%, far more than any interpolation error. Applying the procedure to a real building therefore requires confirmed construction and soil data, a deep-ground temperature justified by site climate, and coordinated temperature and heat-flux measurements.

3. The next step is an annual calculation. ISO 52016-1 and ISO 52017-1 separate time-dependent building calculations from a stationary load [27,28], and ISO 13786 gives dynamic properties of components [29] but not a soil-domain model. Following [6], the transient conduction equation would be integrated implicitly with climate initialisation; this needs climate series, soil heat capacity and moisture data and, for cold regions such as Astana, a treatment of freezing.

REFERENCES

1. International Organization for Standardization. ISO 13370:2017. Thermal performance of buildings – Heat transfer via the ground-Calculation methods. Geneva: ISO; 2017. https://www.iso.org/standard/65716.html

2. International Organization for Standardization. ISO 10211:2017. Thermal bridges in building construction – Heat flows and surface temperatures-Detailed calculations. Geneva: ISO; 2017. https://www.iso.org/standard/65710.html

3. Rees SW, Adjali MH, Zhou Z, Davies M, Thomas HR. Ground heat transfer effects on the thermal performance of earth-contact structures. Renewable and Sustainable Energy Reviews. 2000;4(3):213–265. https://doi.org/10.1016/S1364-0321(99)00018-0

4. Zoras S. A review of building earth-contact heat transfer. Advances in Building Energy Research. 2009;3(1):289–313. https://doi.org/10.3763/aber.2009.0312

5. Malyavina EG, Gnezdilova EA, Levina YN. Influence of thermal insulation of the wall area of the floor on the ground on the heat loss amount. Journal of Physics: Conference Series. 2019;(6):44–48. https://iopscience.iop.org/article/10.1088/1742-6596/1614/1/012062 (In Russ.)

6. Gnezdilova EA. Improving the calculation of heat losses through ground floors with modern insulation structures [Sovershenstvovanie rascheta teplopoter cherez poly po gruntu s sovremennymi construkciamu utepleniya]. Moscow: National Research Moscow State University of Civil Engineering; 2021. (In Russ.) https://www.dissercat.com/content/sovershenstvovanie-rascheta-teplopoter-cherez-poly-po-gruntu-s-sovremennymi-konstruktsiyami

7. Kruis N, Krarti M. Kiva™: a numerical framework for improving foundation heat transfer calculations. Journal of Building Performance Simulation. 2015;8(6):449–468. https://doi.org/10.1080/19401493.2014.988753

8. Kruis N, Krarti M. Three-dimensional accuracy with two-dimensional computation speed: using the Kiva™ numerical framework to improve foundation heat transfer calculations. Journal of Building Performance Simulation. 2017;10(2):161–182. https://doi.org/10.1080/19401493.2016.1211177

9. Neymark J, Judkoff R, Beausoleil-Morrison I, Ben-Nakhi A, Crowley M, Deru M. International Energy Agency Building Energy Simulation Test and Diagnostic Method (IEA

ISSN 3134-8475 (Print)
ISSN 3134-8483 (Online)

BESTEST): In-depth diagnostic cases for ground coupled heat transfer related to slab-on-grade construction. Golden: NREL; 2008. Report NREL/TP-550-43388. https://doi.org/10.2172/937333

10. International Organization for Standardization. ISO 10456:2007. Building materials and products - Hygrothermal properties-Tabulated design values and procedures for determining declared and design thermal values. Geneva: ISO; 2007. https://www.iso.org/standard/40966.html

11. International Organization for Standardization. ISO 6946:2017. Building components and building elements-Thermal resistance and thermal transmittance-Calculation methods. Geneva: ISO; 2017. https://www.iso.org/standard/65708.html

12. SP RK 2.04-01-2017. Building climatology. Astana; 2017. (In Russ.)

13. Patankar SV. Numerical heat transfer and fluid flow. New York: Hemisphere Publishing; 1980. https://doi.org/10.1201/9781482234213

14. Samarskii AA. Theory of difference schemes [Teoriya raznostnyh shem]. 3rd ed. Moscow: Nauka; 1989. https://search.rsl.ru/ru/record/01001539782(In Russ.)

15. Harris CR, Millman KJ, van der Walt SJ, Gommers R, Virtanen P, Cournapeau D, et al. Array programming with NumPy. Nature. 2020;585:357–362. https://doi.org/10.1038/s41586-020-2649-2

16. Virtanen P, Gommers R, Oliphant TE, Haberland M, Reddy T, Cournapeau D, et al. SciPy 1.0: fundamental algorithms for scientific computing in Python. Nature Methods. 2020;17:261–272. https://doi.org/10.1038/s41592-019-0686-2

17. Hunter JD. Matplotlib: a 2D graphics environment. Computing in Science & Engineering. 2007;9(3):90–95. https://doi.org/10.1109/MCSE.2007.55

18. Lykov AV. Theory of heat conduction [Teoriya teploprovodnosti]. Moscow: Vysshaya Shkola; 1967. https://library.bmstu.ru/Catalog/Details/142645(In Russ.)

19. SNiP 2.04.05-91*. Heating, ventilation and air conditioning. Moscow: Gosstroy of the USSR; 1991. (In Russ.)

20. SP RK 2.04-107-2013. Building heat engineering. Astana; 2013. (In Russ.)

21. Celik IB, Ghia U, Roache PJ, Freitas CJ, Coleman H, Raad PE. Procedure for estimation and reporting of uncertainty due to discretization in CFD applications. Journal of Fluids Engineering. 2008;130(7):078001. https://doi.org/10.1115/1.2960953

22. International Organization for Standardization. ISO 9869-1:2014. Thermal insulation—Building elements – In-situ measurement of thermal resistance and thermal transmittance—Part 1: Heat flow meter method. Geneva: ISO; 2014. https://www.iso.org/standard/59697.html

23. International Organization for Standardization. ISO 6781-1:2023. Performance of buildings—Detection of heat, air and moisture irregularities in buildings by infrared methods—Part 1: General procedures. Geneva: ISO; 2023. https://www.iso.org/standard/79848.html

24. Nardi I, Lucchi E, de Rubeis T, Ambrosini D. Quantification of heat energy losses through the building envelope: a state-of-the-art analysis with critical and comprehensive review on infrared thermography. Building and Environment. 2018;146:190–205. https://doi.org/10.1016/j.buildenv.2018.09.050

25. Song A, Kim Y, Hwang S, Shin M, Lee S. A comprehensive review of thermal transmittance assessments of building envelopes. Buildings. 2024;14(10):3304. https://doi.org/10.3390/buildings14103304

26. U.S. Department of Energy. EnergyPlus 24.2 engineering reference: ground heat transfer calculations using Foundation:Kiva [Internet]. 2024 [cited 2026 Nov 18]. https://bigladdersoftware.com/epx/docs/24-2/engineering-reference/ground-heat-transfer-calculations-using-kiva.html

27. International Organization for Standardization. ISO 52016-1:2017. Energy performance of buildings – Energy needs for heating and cooling, internal temperatures and sensible and latent heat loads—Part 1: Calculation procedures. Geneva: ISO; 2017. https://www.iso.org/standard/65696.html

ISSN 3134-8475 (Print)
ISSN 3134-8483 (Online)

28. International Organization for Standardization. ISO 52017-1:2017. Energy performance of buildings – Sensible and latent heat loads and internal temperatures—Part 1: Generic calculation procedures. Geneva: ISO; 2017. https://www.iso.org/standard/65698.html

29. International Organization for Standardization. ISO 13786:2017. Thermal performance of building components – Dynamic thermal characteristics-Calculation methods. Geneva: ISO; 2017. https://www.iso.org/standard/65711.html

ISSN 3134-8475 (Print)
ISSN 3134-8483 (Online)

FUNDING
This research received no external funding.

CONFLICT OF INTEREST
The authors declare no conflict of interest.

ARTIFICIAL INTELLIGENCE STATEMENT
OpenAI ChatGPT was used to assist with drafting and translating the text, writing the Python code, preparing figures and organising references. The authors checked the code, repeated the calculations, verified all results, tables and references, and take full responsibility for the content of the article

INFORMATION ABOUT THE AUTHORS
Ramazan Kuralay Kaiyrgalikyzy – Master's student, International Educational Corporation, Almaty, Kazakhstan, kuralayy07@gmail.com, https://orcid.org/0009-0000-1886-2635
Niyetbay Sayat Erzhanovich – PhD, Associate Professor, School of Construction, International Educational Corporation, Almaty, Kazakhstan. E-mail: sayat_90@inbox.ru. https://orcid.org/0000-0002-9748-6830

AUTHORS CONTRIBUTION
Ramazan K. K. – literature review; research data organisation; numerical analysis; preparation of tables and figures; manuscript drafting and revision.
Niyetbay S. E. – scientific supervision; methodological consultation; critical review and interpretation of results; manuscript review and editing.

The article was submitted 20 July 2026; approved after reviewing 10 August 2026; accepted for publication 25 August 2026.